

# A Diazirine-Modified Membrane Lipid to Study Peptide/Lipid Interactions – Chances and Challenges

Julia Dörner,<sup>[a]</sup> Patricia Korn,<sup>[a]</sup> Kai Gruhle,<sup>[a, b]</sup> Daniel Ramsbeck,<sup>[c, d]</sup> Vasil M. Garamus,<sup>[e]</sup> Hauke Lilie,<sup>[f]</sup> Annette Meister,<sup>[g, h]</sup> Christian Schwieger,<sup>[h]</sup> Christian Ihling,<sup>[a, i]</sup> Andrea Sinz,<sup>[a, i]</sup> and Simon Drescher<sup>\*[b, j]</sup>

**Abstract:** Although incorporation of photo-activatable lipids into membranes potentially opens up novel avenues for investigating interactions with proteins, the question of whether diazirine-modified lipids are suitable for such studies, remains under debate. Focusing on the potential for studying lipid/peptide interactions by cross-linking mass spectrometry (XL-MS), we developed a diazirine-modified lipid (DiazPC), and examined its behaviour in membranes incorporating the model  $\alpha$ -helical peptide LAVA20. We observed an unexpected backfolding of the diazirine-containing stearyl chain of the lipid. This surprising behaviour challenges the potential application of DiazPC for future XL-MS studies of peptide and protein/lipid interactions. The observations made for DiazPC most likely represent a general phenomenon for any type of membrane lipids with a polar moiety incorporated into the alkyl chain. Our finding is therefore of importance for future protein/lipid interaction studies relying on modified lipid probes.

transporters, ion channels, enzymes or receptors. Due to their important metabolic roles, changes in membrane protein structure may therefore cause or promote numerous diseases.<sup>[2]</sup> In addition, 60% of all membrane proteins serve as drug targets,<sup>[3]</sup> and thus a detailed structural elucidation and understanding of a protein's function can aid the design of novel drugs.<sup>[4]</sup>

The methods available for the structural characterization of proteins are diverse, but not all of them are suited to investigate membrane proteins as they require their native environment, viz. membrane lipids, for maintaining their three-dimensional (3D) structure. Although the presence of lipids is essential for some techniques for structural protein analysis, even small amount of lipids could on the other hand interfere with the classical techniques, such as NMR spectroscopy or X-ray diffraction. In recent years, native mass spectrometry (MS) has matured into an alternative method to investigate the 3D-structures of integral membrane proteins.<sup>[5]</sup> However, native MS on membrane proteins requires membrane models mimicking the cellular environment of membrane proteins. In this context, several types of biomimetic lipid assemblies have been employed.<sup>[6]</sup> Another technique among the various structural MS approaches that has come into focus, is chemical cross-linking in combination with MS (XL-MS), as it provides information on the 3D-structure of proteins as well as on

Membrane proteins, comprising ~23% of the human genome,<sup>[1]</sup> play an outstanding role in various cellular processes, acting as

[a] J. Dörner, P. Korn, K. Gruhle, Dr. C. Ihling, Prof. Dr. A. Sinz  
Institute of Pharmacy-Pharmaceutical Chemistry and Bioanalytics  
Martin Luther University (MLU) Halle-Wittenberg  
Kurt-Mothes-Str. 3, 06120 Halle (Saale) (Germany)

[b] K. Gruhle, Dr. S. Drescher  
Institute of Pharmacy-Biophysical Pharmacy  
MLU Halle-Wittenberg  
Wolfgang-Langenbeck-Str. 4, 06120 Halle (Saale) (Germany)  
E-mail: simon.drescher@pharmazie.uni-halle.de

[c] Dr. D. Ramsbeck  
Fraunhofer Institute for Cell Therapy and Immunology IZI  
Weinbergweg 22, 06120 Halle (Saale) (Germany)

[d] Dr. D. Ramsbeck  
Institute of Pharmacy, University Leipzig  
Brüderstr. 34, 04103 Leipzig (Germany)

[e] Dr. V. M. Garamus  
Helmholtz-Zentrum Hereon  
Max-Planck-Str. 1, 21502 Geesthacht (Germany)


[f] Dr. H. Lilie  
Institute for Biochemistry and Biotechnology-Technical Biochemistry  
MLU Halle-Wittenberg  
Kurt-Mothes-Str. 3, 06120 Halle (Saale) (Germany)


[g] Dr. A. Meister  
Institute of Biochemistry and Biotechnology-Physical Biotechnology  
Charles Tanford Protein Center, MLU Halle-Wittenberg  
Kurt-Mothes-Str. 3a, 06120 Halle (Saale) (Germany)

[h] Dr. A. Meister, Dr. C. Schwieger  
Interdisciplinary Research Center HALOmem  
MLU Halle-Wittenberg  
Charles Tanford Protein Center, Kurt-Mothes-Str. 3a, 06120 Halle (Saale)  
(Germany)

[i] Dr. C. Ihling, Prof. Dr. A. Sinz  
Center for Structural Mass Spectrometry  
Kurt-Mothes-Str. 3, 06120 Halle (Saale) (Germany)

[j] Dr. S. Drescher  
Phospholipid Research Center  
Im Neuenheimer Feld 515, 69120 Heidelberg (Germany)

 Supporting information for this article is available on the WWW under <https://doi.org/10.1002/chem.202102048>

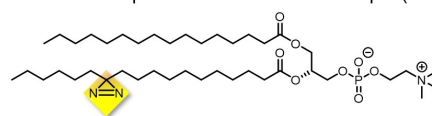
 © 2021 The Authors. Chemistry - A European Journal published by Wiley-VCH GmbH. This is an open access article under the terms of the Creative Commons Attribution Non-Commercial NoDerivs License, which permits use and distribution in any medium, provided the original work is properly cited, the use is non-commercial and no modifications or adaptations are made.

interaction sites between proteins.<sup>[7]</sup> To conduct XL-MS experiments between different proteins, but also between proteins and lipids, several photo-activatable cross-linkers have been developed, containing mainly benzophenone, azide, and diazirine<sup>[8]</sup> moieties. After activation by UV-A light, they form highly reactive carbene and nitrene species, which will non-specifically react with nearly all groups in their immediate vicinity. The protein will thus be covalently connected to either another protein or a lipid. Undoubtedly, the great advantage of XL-MS is its potential to study membrane proteins in their native environment.

Besides adding external cross-linkers, membrane lipids might also be modified and thus serve as reaction partners for membrane proteins. The strategy of inserting a photo-reactive group in the hydrophobic or hydrophilic regions of membrane lipids is not entirely novel<sup>[9]</sup> and pioneering work has been performed by Khorana and co-workers.<sup>[10]</sup> In all previously reported studies, it has been assumed that the physicochemical behaviour of modified and unmodified membrane lipids are entirely comparable, thus ensuring complete miscibility, which is not necessarily the case. We have recently shown that the position of an azide moiety in the alkyl chain of a membrane lipid will indeed influence the type of aggregates formed in aqueous dispersion,<sup>[11]</sup> and affects the miscibility of azide-modified lipids with saturated membrane lipids.<sup>[12]</sup> This highlights the need for more detailed investigations on both aspects of modified lipid behaviour. Although we have demonstrated the general feasibility of using azide-modified lipids for XL-MS studies,<sup>[11,13]</sup> the cross-linking yield of azides was found to be rather low.<sup>[11,14]</sup> We therefore specifically designed a diazirine-modified lipid (DiazPC, Figure 1a) for use in XL-MS studies. The main question to be addressed in peptide/lipid and protein/lipid XL-MS studies is: Is it possible to determine the exact cross-link position between a membrane-embedded peptide (or protein) and a photo-reactive membrane lipid? We sought to address this question by applying a set of physicochemical techniques in combination with XL-MS studies to model membranes containing DiazPC and a transmembrane peptide termed LAVA20 (Figure 1b) which is related to the WAL peptide family.<sup>[15]</sup> XL-MS would provide detailed 3D-structural information on the membrane proteins assembly, such as penetration depth that could be obtained by varying the position of the cross-linker along the lipid alkyl chain (Figure 1c).

The membrane lipid carrying a diazirine moiety in the central part of the alkyl chain, 1-palmitoyl-2-(12,12-diazi-octadecanoyl)-*sn*-glycero-3-phosphocholine (DiazPC), was synthesized from 1,2-dipalmitoyl-*sn*-glycero-3-phosphocholine (DPPC) and 12,12-diazi-octadecanoic acid applying the partial synthetic approach reported previously for the synthesis of modified phospholipids.<sup>[11]</sup> The diazirine-modified fatty acid was in turn prepared from 12-hydroxyoctadecanoic acid using a procedure adapted from Haberkant<sup>[16]</sup> and Church.<sup>[17]</sup> The synthesis is described in the Supporting Information (Scheme S1 and Figures S1 and S2). It is important to note that, after formation of the diazirine group, all following synthesis steps and investigations have to be carried out under red light to prevent inadvertent reactions of the diazirine moiety.

(a) chemical structure of photo-reactive membrane lipid (DiazPC)



(b) LAVA20: Ac-GKKLA<sub>1</sub>VAV<sub>5</sub>LAVAL<sub>10</sub>LAL<sub>15</sub>LWAK<sub>20</sub>-NH<sub>2</sub>

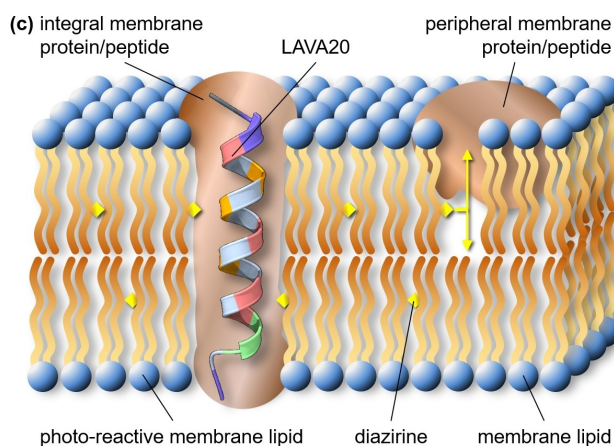


**Figure 1.** (a) Chemical structure of the photo-reactive membrane lipid DiazPC. (b) Sequence of membrane peptide LAVA20 (including colour code of the amino acids). (c) Schematic representation of an integral and peripheral membrane protein or peptide, embedded in a phospholipid bilayer containing DiazPC. The position of the cross-linker (yellow diamonds) can be varied along the alkyl chain.

To enable a reliable 3D-structural characterization of proteins embedded in a lipid bilayer by XL-MS, it was necessary to undertake a detailed study of DiazPC's lyotropic behaviour and its mixing properties with other membrane lipids. When dispersed in water, DiazPC forms an opalescent suspension at room temperature indicating the formation of large lipid assemblies. Transmission electron microscopy (TEM) images (Figure 2a and Figure S6) show very large, stacked lamellar aggregates (> 1  $\mu\text{m}$ ). The differential scanning calorimetry (DSC) heating curve of DiazPC (Figure 2b) shows a broad endothermic transition with a maximum at  $T_m = 16.2^\circ\text{C}$ , which is markedly lower than  $T_m$  of the unmodified counterpart 1-palmitoyl-2-stearoyl-*sn*-glycero-3-phosphocholine (PSPC;  $T_m = 49.0^\circ\text{C}$ ).<sup>[18]</sup> This  $T_m$  decrease is due to the insertion of the diazirine group into the alkyl chain region perturbing their dense packing. Importantly,  $T_m$  of DiazPC is higher than other lipids with symmetry-breaking chain modifications, for example the insertion of one double bond as in 1-palmitoyl-1-oleoyl-*sn*-glycero-3-phosphocholine (POPC;  $T_m = -2.5^\circ\text{C}$ )<sup>[18]</sup> or one azide moiety at position 10 of the stearic acid as in P10AzSPC ( $T_m < 5^\circ\text{C}$ ).<sup>[11]</sup> This could be due to the restricted rotatability at the carbon atom carrying the diazirine group. The thermotropic transition of DiazPC coincides with a fluidization of the alkyl chains, *i.e.* a gel-to-liquid crystalline phase transition as evidenced by infrared (IR) spectroscopic analysis of the temperature-dependent positions of both methylene stretching vibrational bands (Figure 2b and Figure S7a). From the position of the methylene scissoring vibration, we further inferred a hexagonal packing of the alkyl chains (Figure S7b). The small-

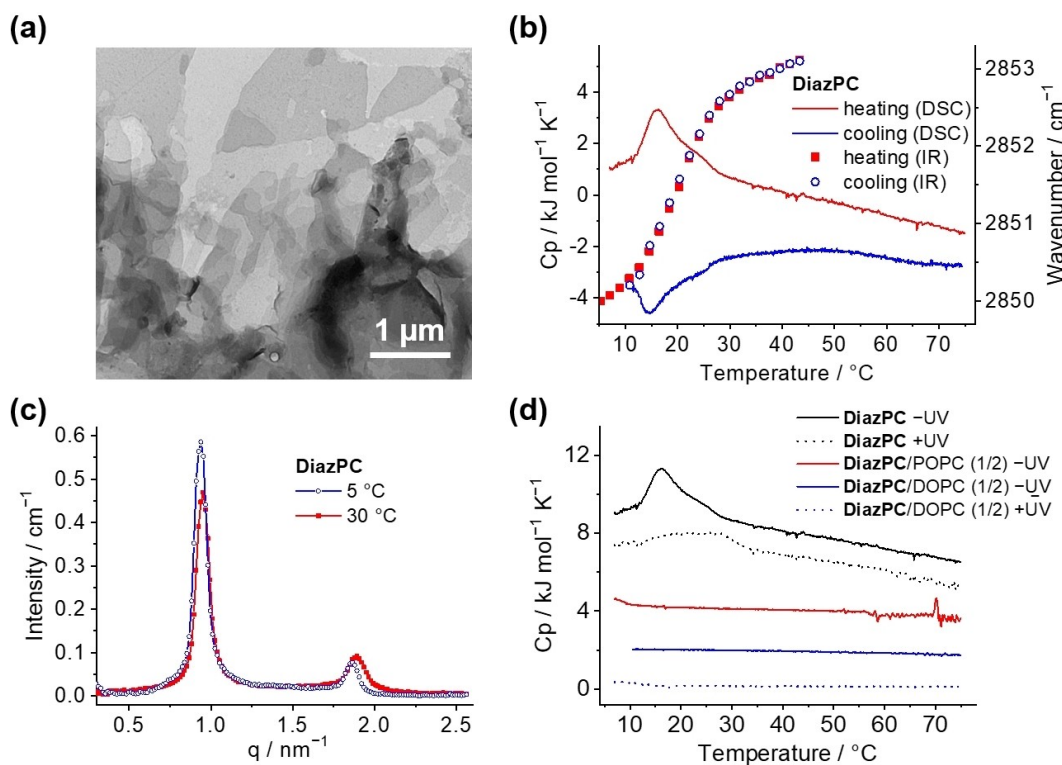


**Figure 2.** (a–c) Data of an aqueous DiazPC suspension: (a) TEM image of a sample ( $c = 0.05 \text{ mg mL}^{-1}$  in water); (b) DSC heating (red line) and cooling (blue line) curve ( $c = 1 \text{ mg mL}^{-1}$  in water) and wavenumber (heating, red squares; cooling, blue squares) of the symmetric methylene stretching vibrational band as a function of temperature ( $c = 100 \text{ mg mL}^{-1}$  in water); (c) SAXS curve at  $5^\circ\text{C}$  (blue) and  $30^\circ\text{C}$  (red) ( $c = 40 \text{ mg mL}^{-1}$  in water). (d) DSC heating curves of lipid mixtures (1/2,  $n/n$ ) containing DiazPC/POPC (red) and DiazPC/DOPC (blue) ( $c_{\text{total}} = 3 \text{ mM}$ ) in phosphate buffer (10 mM, pH 7.5). The DSC curves of pure DiazPC (black) ( $c = 1 \text{ mg mL}^{-1}$ ) is shown for comparison. The dotted lines represent DSC heating curves of samples after UV-A irradiation. The curves are shifted vertically for clarity.

angle X-ray scattering (SAXS) curve of DiazPC at  $5^\circ\text{C}$ , *i.e.* below  $T_m$ , depicts two distinct reflections with equidistant spacing at  $q_1 = 0.94 \text{ nm}^{-1}$  and  $q_2 = 1.86 \text{ nm}^{-1}$  (Figure 2c and Table S1). These values correspond to a lamellar repeat distance of  $d = 6.7 \pm 0.1 \text{ nm}$ . Above  $T_m$  (at  $30^\circ\text{C}$ ), the repeat distance slightly decreases to  $d = 6.6 \pm 0.1 \text{ nm}$  (Figure 2c), due to the increased number of *gauche* conformers in the alkyl chains shortening their effective length. Thus, DiazPC behaves quite comparably to other membrane-forming phospholipids<sup>[18]</sup> except for the particular  $T_m$  value observed by DSC and IR.

Since biological membranes are in the liquid-crystalline state at room temperature, mixing studies were performed with the unsaturated lipids POPC and 1,2-dioleoyl-*sn*-glycero-3-phosphocholine (DOPC) both of which have  $T_m$  below  $0^\circ\text{C}$ .<sup>[18]</sup> In the corresponding mixtures including 33 mol% DiazPC, no transition peak was found between  $5\text{--}75^\circ\text{C}$ , indicating complete miscibility of the respective lipid components at this mixing ratio—an indispensable prerequisite for doping model membranes with photo-reactive lipids for further lipid/protein interaction studies. In the case of partial or complete demixing, we would expect a transition peak of the lipid mixture in close proximity to  $T_m$  of the pure DiazPC. After UV-A irradiation of pure DiazPC, its DSC transition slightly shifted to higher temperatures and the peak became broader (Figure 2d, dotted lines). This indicates the occurrence of new lipid species

resulting in structural rearrangement of lipids within the bilayer membrane. Theoretically, the same should also occur in the DiazPC/DOPC mixtures, however, after UV-A irradiation, again no transition was observed for this mixture, implying no changes in the phase state of the mixed membrane.

To test the applicability of DiazPC for the XL-MS approach, we used the  $\alpha$ -helical peptide LAVA20 (Figure 1b, Figures S3–S5). LAVA20 is a modified version of the established transmembrane model peptides WALP and KALP, which have been widely studied by Killian and co-workers.<sup>[15a,19]</sup> LAVA20 contains two lysine residues at the N-terminus and one lysine residue at the C-terminus to ensure formation of charged fragment ions during subsequent MS analysis. DiazPC/DOPC liposomes incorporating 2 mol% LAVA20 were characterized using dynamic light scattering (DLS) and TEM (Figures 3a–c) showing a monomodal distribution of liposome diameters with a maximum at  $124 \pm 2 \text{ nm}$ . The concentration of LAVA20 in the liposomes was determined by the absorption of tryptophan at  $\lambda = 280 \text{ nm}$  (Figure 3d). With knowledge of the exact concentration of LAVA20 ( $c_{\text{LAVA20}} = 0.38 \pm 0.01 \text{ mM}$ ), the helical structure of LAVA20 was confirmed by circular dichroism (CD) spectroscopy (Figure 3d).<sup>[20]</sup> Here, the typical minima for helical structures are clearly visible at 209 and 222 nm as well as the pronounced maximum at 192 nm. Using the CDNN database software,<sup>[21]</sup> 60%  $\alpha$ -helical structure content was calculated

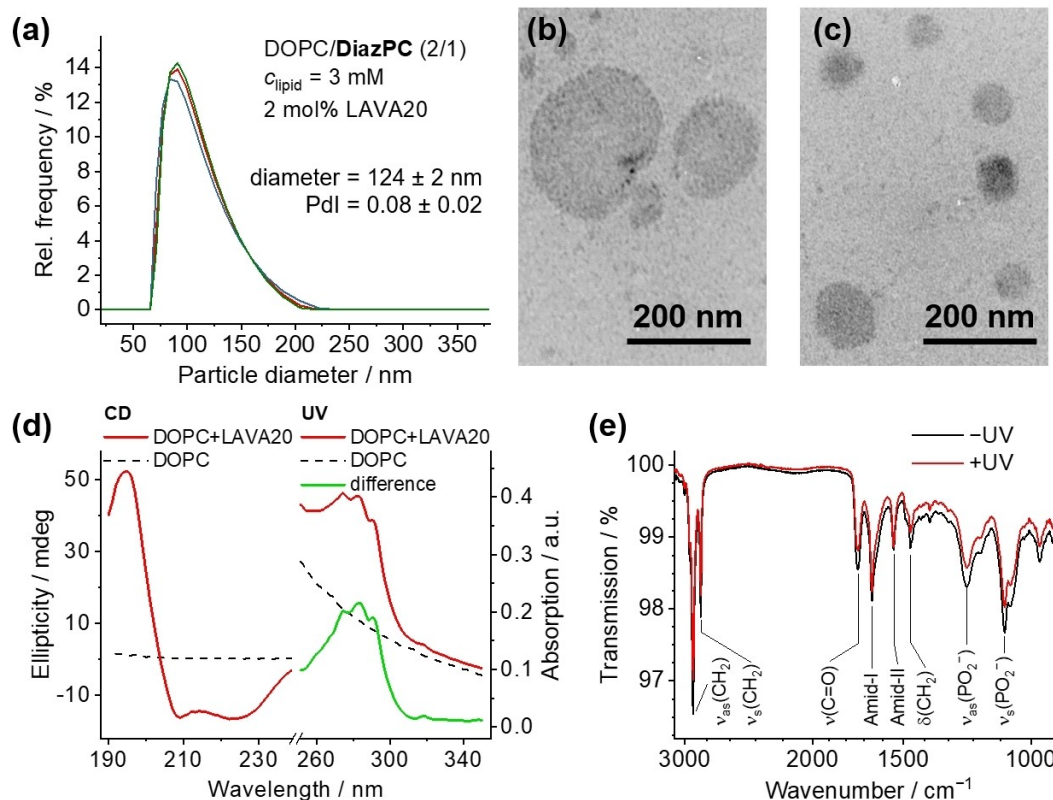


**Figure 3.** (a) Volume-weight particle size distribution (determined by DLS) of DiazPC/DOPC (1/2,  $n/n$ ) liposomes incorporating 2 mol% LAVA20 ( $c_{\text{lipid}} = 3 \text{ mM}$ ) prepared with freeze/thaw cycles followed by extrusion ( $n = 3$ ). (b–c) TEM images of aqueous DiazPC/DOPC (1/2) suspensions ( $c_{\text{lipid}} = 60 \mu\text{M}$ ) including 2 mol% LAVA20, prior to (b) and after (c) UV irradiation. (d) CD (left) and UV spectra (right) of pure DOPC liposomes (black dashed line), DOPC liposomes including 2 mol% LAVA20 (red solid line), and the difference of both (UV, green solid line);  $c_{\text{DOPC}} = 1.15 \text{ mg mL}^{-1}$ ,  $c_{\text{LAVA20}} = 0.38 \pm 0.01 \text{ mM}$ . The LAVA20-containing liposomes were prepared in PB (10 mM, pH 7.4). (e) ATR-IR spectra of DiazPC/DOPC (1/2,  $n/n$ ;  $c = 3 \text{ mM}$  in PBS, pH 7.4) vesicles including 2 mol% LAVA20 prior to (black) and after (red) UV-A irradiation.

indicating that the membrane-bound segment, containing the lipophilic amino acids leucine, alanine, and valine, exhibits the desired  $\alpha$ -helical structure, while the polar terminal regions possess a non-helical structure containing 25% random coil, 12%  $\beta$ -sheet, and other structures. To examine possible denaturation of the peptide during the cross-linking experiments, attenuated total reflection (ATR)-IR measurements were performed prior to and after UV-A irradiation (Figure 3e). The position of the amide I band at  $1657 \text{ cm}^{-1}$  and the amide II band at  $1547 \text{ cm}^{-1}$  confirmed the  $\alpha$ -helical structure of LAVA20 prior to and after UV-A irradiation.<sup>[22]</sup> Absorption bands originating from the lipid components were also visible. Changes in the position of these bands would provide evidence for phenomena such as phase transitions of lipids or alterations to hydration of the lipid headgroups. Since the spectra prior to and after UV exposure were identical, any denaturation of LAVA20 or conformational changes of lipids caused by irradiation could be excluded, reinforcing the applicability of this approach.

The photoreaction of diazirines has been widely described in the literature<sup>[17,23]</sup> and is further detailed in the Supporting Information (Scheme S2). After UV irradiation at  $\lambda = 365 \text{ nm}$ , the generated carbene, which has only a short half-life in the range of pico- to nanoseconds,<sup>[24]</sup> will react non-specifically with

amino acid residues of membrane peptides/proteins, with adjacent lipids, or simply with water. Recent studies have shown a preferred reactivity of diazirines with carboxylic acids that proceeds via linearization to diazo compounds.<sup>[25]</sup> Moreover, degradation products might be formed, of which the mono-unsaturated C18 acids exhibit an identical molecular weight to oleic acid in POPC, making it challenging to discriminate these degradation products from POPC in MS. Therefore, DOPC was used in the XL-MS studies instead.

We applied MS to monitor the time course of DiazPC degradation and peptide/lipid cross-link formation based on their MS signal intensities relative to that of DOPC. The cross-linked product between DiazPC and LAVA20 appeared as a triply charged ion at  $m/z 960.632$ , corresponding to  $[\text{DiazPC} + \text{LAVA20} - \text{N}_2 + 3\text{H}]^{3+}$  (Figures 4a and b). The DiazPC signal had almost disappeared after 25 s of UV-A irradiation, while MS signal intensity of the cross-linked product steadily increased over time (Figure 4c). The total ion chromatogram (TIC) of DiazPC/DOPC liposomes spiked with 2 mol% LAVA20 shows four main MS signals prior to UV-A irradiation (Figure 4d and Table S2): LAVA20, DiazPC, DOPC, PSPC, the latter being a side product of DiazPC synthesis. After UV-A irradiation, the signal intensities of LAVA20 and DiazPC decreased and several new signals emerged. In addition to the DiazPC/LAVA20 cross-link, a

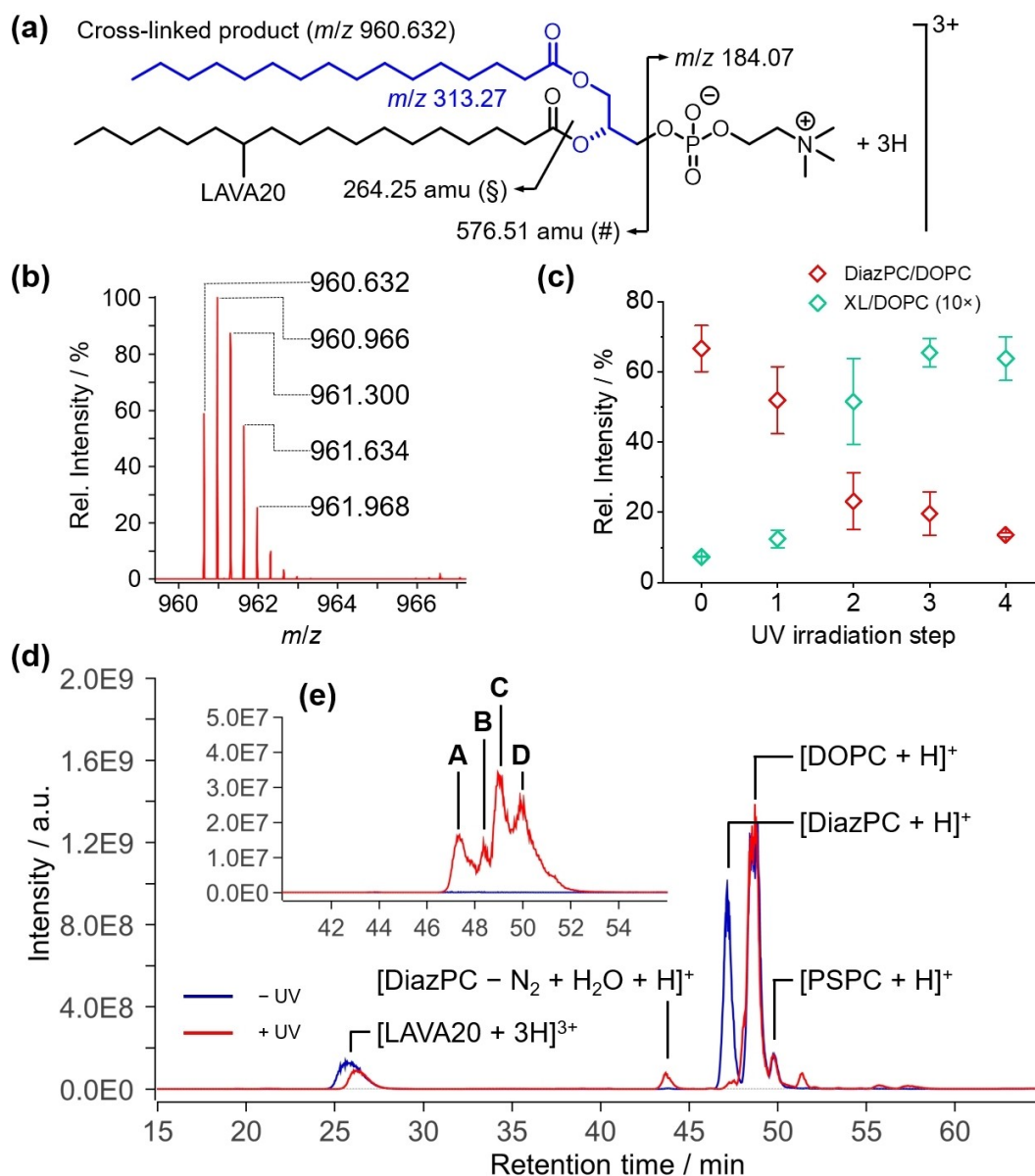


**Figure 4.** (a) Chemical structure of the cross-linked product between DiazPC and LAVA20 after UV-A activation ( $\lambda = 365$  nm) and nitrogen loss. Specific fragmentations at the lipid and mass differences of LAVA20 (# and §) were observed as indicated. (b) Mass spectrum of the triply charged cross-linked product [ $\text{DiazPC} + \text{LAVA20} - \text{N}_2 + 3\text{H}$ ] $^{3+}$  at  $m/z$  960.632. (c) Intensities of DiazPC (red) and the cross-linked (XL) product (green, 10x) relative to the intensity of DOPC after different (additive) UV-A irradiation conditions: step 1 = 2 s at 10% of max. power, 2 = 20 s at 10%, 3 = 0.2 s at 100%, and 4 = 2 s at 100% ( $n=4$ , mean and SD are given). (d) TIC of DiazPC/DOPC (1/2) vesicles including 2 mol% LAVA20 prior to (blue) and after (red) UV-A irradiation. (e) Extracted ion chromatograms of the cross-linked product prior to (blue) and after (red) UV-A irradiation.

decomposition product of DiazPC was visible due to the reaction of the generated carbene with water as well as a cross-link between DiazPC and DOPC. Interestingly, the DiazPC/LAVA20 cross-link showed four clearly distinguishable retention times ( $t_R$ ) as shown in the extracted ion chromatogram (Figure 4e).

To further address why the cross-linked product at  $m/z$  960.632 exhibits a distinct chromatographic behaviour and to locate the exact cross-link position, MS/MS experiments were performed on each sub-species. In all four fragment ion mass spectra, a species at  $m/z$  313.273 was identified, corresponding

to the cleavage of the lipid's PC headgroup ( $m/z$  184.072) and the modified stearic acid (Figure 4a, structure highlighted in blue). A number of signals, especially in the lower  $m/z$  range, were assigned to internal fragment ions originating from double cleavage of the peptide backbone (Table S3, Table S4). These species did not show any modification resulting from the cross-linking reaction with DiazPC. In the higher  $m/z$  range, mass spectra of peaks A (Figure 5a) and D (Figure S9) gave completely identical fragment ions only slightly differing in signal intensities. In both cases, a series of unmodified  $y$ -type ions ( $y_3^+$  to  $y_{18}^+$ ) was observed originating from cleavage of the

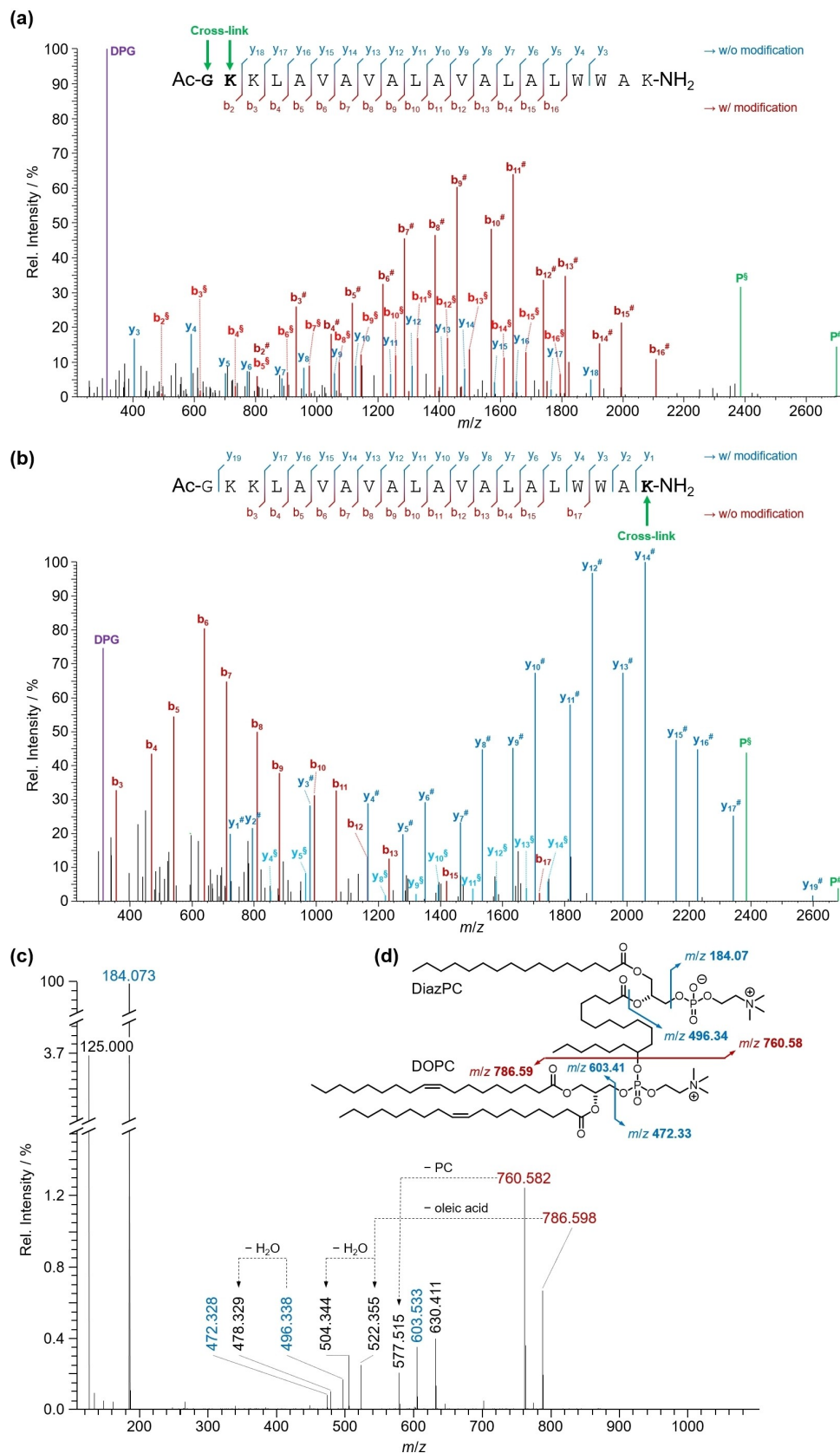


**Figure 5.** (a–b) Deconvoluted and deisotoped fragment ion mass spectrum of cross-linked product at  $m/z$  960.632 at (a)  $t_R = 47.2$ – $47.6$  min (peak A of Figure 4e) and at (b)  $t_R = 48.3$ – $48.5$  min (peak B of Figure 4e). DPG, 3-deoxy-1-palmitoyl-glycerol; P, precursor; #, [fragment ion–phosphocholine]; S, [fragment ion–1-palmitoyl-*sn*-glycero-3-phosphocholine]. (c) Fragment ion mass spectrum of the DiazPC/DOPC cross-linked product at  $m/z$  773.592. (d) Chemical structure of the DiazPC/DOPC cross-linked product, specific fragment ions are indicated.

peptide bonds of LAVA20. In contrast, b-type ions ( $b_2^+$  to  $b_{16}^+$ ) carried a modification with a mass difference of 576.51 amu (#) corresponding to the cross-linked lipid fragment that remains attached to the peptide after cleavage of the lipid PC headgroup. Another modification was observed corresponding to cleavage of the stearic acid ester bond and formation of a ketone, resulting in a mass difference of 264.25 amu (\$). This clearly identifies the cross-link position at the two N-terminal amino acids of the LAVA20 peptide ( $G_1$  or  $K_2$ ).

The fragment ion spectra of peaks B (Figure 5b) and C (Figure S8) also agreed with each other, but they differ clearly from the spectra of peaks A and D. Strikingly, the b-type ion series  $b_3^+$  to  $b_{17}^+$  was observed without modifications. However, a mass difference of 576.51 amu (#) and of 264.25 amu (\$) was found for the peptide backbone fragment ions  $y_1^+$  to  $y_{19}^+$  and  $y_4^+$  to  $y_{14}^+$ , respectively. Hence, this cross-linked product must be modified at the C-terminal lysine ( $K_{20}$ ) of the LAVA20 sequence. The four different retention times are indicative of cluster formation, *i.e.*, the formation of molecular aggregates stabilized by non-covalent interactions.<sup>[26]</sup> During the electrospray ionization, these non-covalent interactions were cleaved releasing individual molecules and, hence, two of the fragment ion spectra were identical in each case (A/D and B/C).

In addition to DiazPC/LAVA20 cross-links, we also identified a cross-link between DiazPC and DOPC at  $m/z$  773.592. In the corresponding fragment ion mass spectrum, the peak of the PC headgroup ( $m/z$  184.072) was identified as base peak (Figure 5c). With lower signal intensities, other fragments emerged including singly charged ions at  $m/z$  786.598 and 760.582. These two ions were formed by cleavage of the cross-link. Since C–C bonds cannot be cleaved by the collisional activation conditions applied herein, cross-link product formation involving the headgroup of DOPC was confirmed (Figure 5d), most likely resulting in a phosphoric acid diester.<sup>[25]</sup> Formation of this specific cross-link requires the diazirine to be in close proximity to the DOPC headgroup, *i.e.*, in the hydrophilic region of the lipid bilayer.

The fact that we detected only cross-links at the C- and N-termini of LAVA20 as well as between DiazPC and the headgroup of DOPC allowed us to unambiguously conclude that the diazirine group of DiazPC is located in the hydrophilic headgroup region of the lipid bilayer (Figure 6). This is caused by the polarity of the diazirine moiety<sup>[27]</sup> and the high flexibility of the lipid alkyl chain allowing its backfolding to the membrane interface. Assuming an unfolded alkyl chain and a positioning of the diazirine group in the hydrophobic region instead, cross-links between DiazPC and LAVA20 within the  $\alpha$ -helix as well as a collisional fragmentation persistent cross-link between DiazPC and DOPC would be expected, neither of which was the case.

In summary, we demonstrate that DiazPC fulfils all prerequisites for a photo-activatable membrane lipid to study protein/lipid interactions: The aggregation behaviour of DiazPC is comparable to other membrane lipids, it is miscible with unsaturated phospholipids, UV-A activation does not influence the membrane organization and generates cross-links between

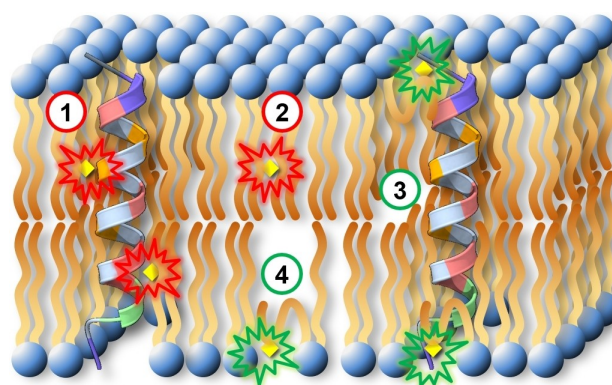


**Figure 6.** Schematic representation of LAVA20 embedded in a lipid bilayer bearing DOPC and DiazPC. The photo-reactive diazirine group (yellow diamonds) is located either within the hydrophobic part of the bilayer (cases 1 and 2) or in the hydrophilic headgroup region (cases 3 and 4) due to back-folding of the *sn*-2 alkyl chain of the DiazPC. Cases 1 and 2 were experimentally not found, while cases 3 and 4 were verified in our study.

DiazPC and surrounding molecules such as peptides or membrane lipids, and the exact position of these peptide/lipid cross-links can be identified using MS. However, due to the backfolding of the modified lipid alkyl chain exclusively cross-links in the headgroup region of the bilayer will be formed. We believe that this is a general feature of alkyl chain-modified phospholipids if the modification is hydrophilic. In these cases, this modification will most likely be located close to the headgroups of a bilayer of the membrane lipids in the liquid-crystalline state. This finding is of major importance for future experiments relying on modified membrane lipids to study peptide/lipid and protein/lipid interactions since the way these studies have been performed so far does not lead to success. Therefore, ways must be found to prevent the backfolding of the lipid alkyl chain.

## Acknowledgements

This work was financially supported by the DFG (project Si 867/15-2 to A.S.). The support of Dr. Gerd Hause (Martin Luther University Halle-Wittenberg) by providing us access to the electron microscope facility is greatly appreciated. The authors thank Dr. Sindy Müller and Dr. Rico Schmidt for their support during physicochemical and MS investigations, respectively, and Dr. Richard Harvey (University of Vienna) for critical reading of the manuscript. Open Access funding enabled and organized by Projekt DEAL.

## Conflict of Interest

The authors declare no conflict of interest.

**Keywords:** diazine · mass spectrometry · membrane lipids · miscibility · peptide/lipid interactions · photo-cross-linking · XL-MS

- [1] M. Uhlen, L. Fagerberg, B. M. Hallstrom, C. Lindskog, P. Oksvold, A. Mardinoglu, A. Sivertsson, C. Kampf, E. Sjostedt, A. Asplund, I. Olsson, K. Edlund, E. Lundberg, S. Navani, C. A. Szgyarto, J. Odeberg, D. Djureinovic, J. O. Takanen, S. Hober, T. Alm, P. H. Edqvist, H. Berling, H. Tegel, J. Mulder, J. Rockberg, P. Nilsson, J. M. Schwenk, M. Hamsten, K. von Feilitzen, M. Forsberg, L. Persson, F. Johansson, M. Zwahlen, G. von Heijne, J. Nielsen, F. Ponten, *Science* **2015**, *347*, 1260419.
- [2] D. L. Stokes, W. J. Rice, M. Hu, C. Kim, I. Ubarretxena-Belandia, *Methods Mol. Biol.* **2010**, *654*, 187–205.
- [3] J. P. Overington, B. Al-Lazikani, A. L. Hopkins, *Nat. Rev. Drug Discovery* **2006**, *5*, 993–996.
- [4] H. Yin, A. D. Flynn, *Annu. Rev. Biomed. Eng.* **2016**, *18*, 51–76.
- [5] a) J. Bender, C. Schmidt, *Biol. Chem.* **2019**, *400*, 813–829; b) J. R. Bolla, M. T. Agasid, S. Mehmood, C. V. Robinson, *Annu. Rev. Biochem.* **2019**, *88*, 85–111.
- [6] a) A. N. Calabrese, T. G. Watkinson, P. J. F. Henderson, S. E. Radford, A. E. Ashcroft, *Anal. Chem.* **2015**, *87*, 1118–1126; b) F. Hagn, M. Etzkorn, T. Raschle, G. Wagner, *J. Am. Chem. Soc.* **2013**, *135*, 1919–1925; c) A. O. Oluwole, B. Danielczak, A. Meister, J. O. Babalola, C. Vargas, S. Keller, *Angew. Chem. Int. Ed.* **2017**, *56*, 1919–1924; *Angew. Chem.* **2017**, *129*, 1946–1951; d) N. Hellwig, O. Peetz, Z. Ahdash, I. Tascon, P. J. Booth, V. Mikusevic, M. Diskowski, A. Politis, Y. Hellmich, I. Hanelt, E. Reading, N. Morgner, *Chem. Commun.* **2018**, *54*, 13702–13705; e) J. T. Hopper, Y. T. Yu, D. Li, A. Raymond, M. Bostock, I. Liko, V. Mikhailov, A. Laganowsky, J. L. Benesch, M. Caffrey, D. Nietlispach, C. V. Robinson, *Nat. Methods* **2013**, *10*, 1206–1208; f) E. Henrich, O. Peetz, C. Hein, A. Laguerre, B. Hoffmann, J. Hoffmann, V. Dotsch, F. Bernhard, N. Morgner, *eLife* **2017**, *6*, e20954; g) C. Sahin, D. J. Reid, M. T. Marty, M. Landreh, *Biochem. Soc. Trans.* **2020**, *48*, 547–558; h) M. Frick, C. Schwieger, C. Schmidt, *Angew. Chem. Int. Ed.* **2021**, *60*, 11523–11530.
- [7] a) C. Arlt, M. Götze, C. H. Ihling, C. Hage, M. Schäfer, A. Sinz, *Anal. Chem.* **2016**, *88*, 7930–7937; b) A. Sinz, *Angew. Chem. Int. Ed.* **2018**, *57*, 6390–6396; *Angew. Chem.* **2018**, *130*, 6498–6504.
- [8] a) J. Brunner, *Annu. Rev. Biochem.* **1993**, *62*, 483–514; b) S. H. Giese, A. Belsom, J. Rappsilber, *Anal. Chem.* **2016**, *88*, 8239–8247.
- [9] a) C. Thiele, M. J. Hannah, F. Fahrenholz, W. B. Huttner, *Nature Cell. Biol.* **2000**, *2*, 42–49; b) A. N. Ridder, R. E. Spelbrink, J. A. Demmers, D. T. Rijkers, R. M. Liskamp, J. Brunner, A. J. Heck, B. de Kruijff, J. A. Killian, *Biochem.* **2004**, *43*, 4482–4489.
- [10] a) R. Radhakrishnan, C. E. Costello, H. G. Khorana, *J. Am. Chem. Soc.* **1982**, *104*, 3990–3997; b) G. E. Gerber, R. Radhakrishnan, C. M. Gupta, H. G. Khorana, *Biochim. Biophys. Acta* **1981**, *640*, 646–654; c) B. Erni, H. G. Khorana, *J. Am. Chem. Soc.* **1980**, *102*, 3888–3896; d) P. Chakrabarti, H. G. Khorana, *Biochem.* **1975**, *14*, 5021–5033.
- [11] S. Lindner, K. Gruhle, R. Schmidt, V. M. Garamus, D. Ramsbeck, G. Hause, A. Meister, A. Sinz, S. Drescher, *Langmuir* **2017**, *33*, 4960–4973.
- [12] S. Müller, C. Schwieger, K. Gruhle, V. M. Garamus, G. Hause, A. Meister, S. Drescher, *Langmuir* **2019**, *35*, 12439–12450.
- [13] M. Hoffmann, S. Drescher, C. Ihling, D. Hinderberger, C. Schwieger, *Langmuir* **2020**, *36*, 12804–12815.
- [14] a) A. Sinz, S. Kalkhof, C. Ihling, *J. Am. Soc. Mass Spectrom.* **2005**, *16*, 1921–1931; b) K. Kölbl, C. H. Ihling, A. Sinz, *Angew. Chem. Int. Ed.* **2012**, *51*, 12602–12605; *Angew. Chem.* **2012**, *124*, 12770–12774.
- [15] a) A. Holt, L. Rougier, V. Reat, F. Jolibois, O. Saurel, J. Czaplicki, J. A. Killian, A. Milon, *Biophys. J.* **2010**, *98*, 1864–1872; b) T. C. Anglin, K. L. Brown, J. C. Conboy, *J. Struct. Biol.* **2009**, *168*, 37–52.
- [16] P. Haberkant, R. Raijmakers, M. Wildwater, T. Sachsenheimer, B. Brügger, K. Maeda, M. Houweling, A. C. Gavin, C. Schultz, G. van Meer, A. J. Heck, J. C. Holthuis, *Angew. Chem. Int. Ed.* **2013**, *52*, 4033–4038; *Angew. Chem.* **2013**, *125*, 4125–4130.
- [17] R. F. R. Church, A. S. Kende, M. J. Weiss, *J. Am. Chem. Soc.* **1965**, *87*, 2665–2671.
- [18] R. Koynova, M. Caffrey, *Biochim. Biophys. Acta Rev. Biomembr.* **1998**, *1376*, 91–145.
- [19] a) J. A. Killian, *FEBS Lett.* **2003**, *555*, 134–138; b) M. R. de Planque, J. A. W. Kruijter, R. M. J. Liskamp, D. Marsh, D. V. Greathouse, R. E. Koeppe II, B. de Kruijff, J. A. Killian, *J. Biol. Chem.* **1999**, *274*, 20839–20846.
- [20] W. C. Johnson, *Annu. Rev. Biophys. Biophys. Chem.* **1988**, *17*, 145–166.
- [21] G. Böhm, R. Muhr, R. Jaenicke, *Protein Eng. Des. Sel.* **1992**, *5*, 191–195.
- [22] J. Kong, S. Yu, *Acta Biochim. Biophys. Sin.* **2007**, *39*, 549–559.
- [23] a) H. M. Frey, I. D. R. Stevens, *J. Chem. Soc.* **1964**, 4700–4706; b) R. F. R. Church, M. J. Weiss, *J. Org. Chem.* **1970**, *35*, 2465–2471.
- [24] a) J. R. Hill, A. A. B. Robertson, *J. Med. Chem.* **2018**, *61*, 6945–6963; b) R. A. Moss, *Acc. Chem. Res.* **2006**, *39*, 267–272.
- [25] a) C. Iacobucci, M. Gotze, C. Piotrowski, C. Arlt, A. Rehkamp, C. Ihling, C. Hage, A. Sinz, *Anal. Chem.* **2018**, *90*, 2805–2809; b) A. V. West, G. Muncipinto, H.-Y. Wu, A. C. Huang, M. T. Labenski, L. H. Jones, C. M. Woo, *J. Am. Chem. Soc.* **2021**, *143*, 6691–6700.
- [26] S. H. Giese, A. Belsom, L. Sinn, L. Fischer, J. Rappsilber, *Anal. Chem.* **2019**, *91*, 2678–2685.
- [27] a) L. Pierce, S. V. Dobyns, *J. Am. Chem. Soc.* **1962**, *84*, 2651–2652; b) C. Puzzarini, A. Gambi, G. Cazzoli, *J. Mol. Struct.* **2004**, *695–696*, 203–210.

Manuscript received: June 10, 2021

Accepted manuscript online: August 18, 2021

Version of record online: September 28, 2021